VIBRONIC EFFECTS IN EPR SPECTRA OF $(NH_4)_2Cu(BeF_4)_2 \cdot 6H_2O$ SINGLE CRYSTAL

S.K. HOFFMANN AND M. GOMÓLKA-MARCINIAK

Institute of Molecular Physics, Polish Academy of Sciences
Smoluchowskiego 17/19, 60-179 Poznań, Poland

(Received March 4, 1993; in final form April 6, 1993)

Angular variations of the g-factors and linewidth value were recorded at X-band, at room temperature, and at 77 K. The temperature dependence of the g-factors was measured along the principal g-tensor axes in the temperature range from 4.2 K to 300 K. The rigid lattice g-factors at 4.2 K are: $g_x = 2.428$, $g_y = 2.138$, and $g_z = 2.058$. The g_x value very slowly increases linearly on heating, whereas g_z and g_y nonlinearly tend towards their average value. This is a typical behaviour of Cu(II) EPR in Tutton salt crystals, however the $g(T)$ dependence is much less pronounced in $(NH_4)_2Cu(BeF_4)_2 \cdot 6H_2O$ as compared to the Cu(II) doped salts. The results are described in terms of the two vibronic coupling models of the strong Jahn–Teller effect. It is shown that the models are not adequate to describe the vibronic g-factor behaviour in paramagnetic Cu(II) crystals which is attributed to the cooperative Jahn–Teller effect existing in these crystals.

PACS numbers: 76.30–v, 71.70.Ej

1. Introduction

The Tutton salts form an isostructural series of monoclinic crystals of the general formula $M'_2M''A_2 \cdot 6H_2O$, where $M' = NH_4$, K, Rb, Cs, Tl; $M'' =$ Zn, Cu, Cd, Co, Mn, Ni and $A = SO_4$, SeO_4, BeF_4, with very close crystal unit cell dimensions within the whole family and $a : b : c$ ratio approximately equal to 3 : 4 : 2, and monoclinic angle $\beta = 105°$ [1]. Since the pioneering work of Bleaney et al. [2] there is a constant interest in EPR studies of paramagnetic Cu(II) Tutton salts as well as of diamagnetic salts doped with copper(II) ions. It is because of their interesting dynamic properties related to the Jahn–Teller type effect of octahedral $[Cu(H_2O)_6]$ complexes [3, 4] which can be rationalized in terms of a fluxional behaviour of the CuO_6-chromophore [5].

The octahedral $[Cu(H_2O)_6]^{2+}$ ions are highly axially distorted both in copper(II) salts and in Cu(II) doped Zn and Cd salts, whereas $[Zn(H_2O)_6]$ and $[Cd(H_2O)_6]$ octahedrons are only slightly distorted from ideal O_h symmetry. It

proves that the $[Cu(H_2O)_6]^{2+}$ distortion is due to a strong Jahn–Teller effect and stabilized by the lattice forces.

Structural and EPR data are available mainly for sulphate Cu(II) Tutton salts. In all Tutton salts of alkali metals the octahedra are elongated along the Cu–O(8) bond, according to the crystallographic notation [6], whereas in $(NH_4)_2Cu(SO_4)_2 \cdot 6H_2O$ the octahedron elongation appears along the Cu–O(7) bond which can be due to the hydrogen bonds between NH_4^+ ions and coordinated water molecules. The Cu–O distances continuously increase on cooling demonstrating the complex fluxional behaviour and the values of the Cu–O bond lengths are determined by a balance between dynamical Jahn–Teller forces and lattice strains, although some contributions from a cooperative Jahn–Teller type interaction between Cu(II) complexes can be expected [7].

A characteristic feature of the EPR of Cu(II) ions in the Tutton salt crystals is that the g-factors and hyperfine splittings are temperature dependent for admixture Cu(II) ions, whereas for the Cu(II) salts the g-factors are practically temperature insensitive with exception of $(NH_4)_2Cu(SO_4)_2 \cdot 6H_2O$ where such dependence was reported [6, 7]. The g-factors exhibit a vibronic type behaviour (pseudo-Jahn–Teller effect) with an averaging tendency for the two larger g-factors (g_z and g_y) on heating, whereas the g_x value appearing along the shortest Cu–O(9) bond only weakly increases with temperature. This behaviour was described in terms of two models: as a result of variations in the thermal population of the either energetically inequivalent potential wells or vibronic levels, as will be described in the next section.

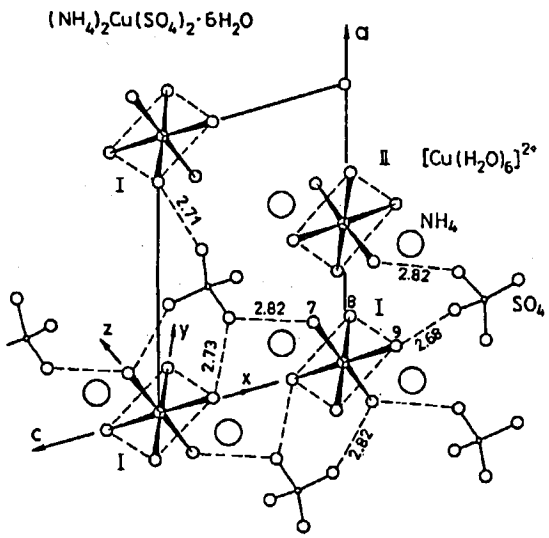

Fig. 1. Unit cell projection of $(NH_4)_2Cu(SO_4)_2 \cdot 6H_2O$ crystal along the (010) direction. Two magnetically inequivalent $[Cu(H_2O)_6]^{2+}$ octahedra 1 and 2 are marked consistently with EPR anisotropy data (Fig. 4).

In this paper we will present the results of detailed EPR studies of $(NH_4)_2Cu(BeF_4)_2 \cdot 6H_2O$ single crystals which have not been studied so far. The details of the crystal structure are not available for this compound and only the unit cell dimensions are known to be: $a = 0.9213$, $b = 1.2417$, $c = 0.6227$ nm, and $\beta = 105.95°$ with $Z = 2$ in $P2_1/c$ space group [8]. These parameters are typical of the Tutton salt crystals and are comparable to those determined for $(NH_4)_2Cu(SO_4)_2 \cdot 6H_2O$: $a = 0.9216$, $b = 1.2398$, $c = 0.6301$ nm, and $\beta = 106.12°$, $P2_1/a$ [9]. The question is whether the $[Cu(H_2O)_6]$ octahedron in $(NH_4)_2Cu(BeF_4)_2 \cdot 6H_2O$ structure is deformed along Cu–O(8) bond as in most of the Cu(II) Tutton salts or along Cu–O(7) bond as it was found in $(NH_4)_2Cu(SO_4)_2 \cdot 6H_2O$ (Fig. 1). The question has no obvious answer, since more stronger hydrogen bonds between fluorine atoms and water molecules are expected and indeed observed in fluoroberyllates [10], and moreover a weakening of the hydrogen bonds in $(ND_4)_2Cu(SO_4)_2 \cdot 6D_2O$ results in a switching of the elongation direction from Cu–O(7) to Cu–O(8) bond [1]. We will discuss and answer this question on the basis of our EPR data. Moreover, in our preliminary studies of the $(NH_4)_2Cu(BeF_4)_2 \cdot 6H_2O$ crystal [11] we have found a vibronic g-factor behaviour, which is however, much weaker as compared to that found in $(NH_4)_2Cu(SO_4)_2 \cdot 6H_2O$ [7]. We will describe this behaviour in terms of the existing models and discuss their validity in condensed Cu(II) paramagnets.

2. Experimental

Crystals of $(NH_4)_2Cu(BeF_4)_2 \cdot 6H_2O$ were prepared by crystallization of a water solution of the ammonium fluoroberyllate, copper carbonate, and hydrofluoric acid. Dark blue crystals were obtained after few days of standing at room temperature and were found to have a satisfactory chemical analysis. The crystals grow in two morphological forms: in the typical form of the Tutton salt crystals with a, b-plane and (110)-planes being well developed, and as rods elongated along [001] direction with well developed (010) plane.

EPR spectra were recorded on a RADIOPAN SE/X-2547 spectrometer operating at X-band with a rectangular TE_{102} cavity and 100 kHz magnetic modulation in the temperature range from 4.2 K to room temperature. Angular variations of the single crystal EPR spectra were measured in the orthogonal reference frame 1, 2, 3 with $1 \equiv a \times b = c^*$, $2 \equiv -b$, $3 \equiv a$.

3. Effects of the vibronic coupling in Cu(II) EPR spectra

Vibronic interactions between electron and nuclear motions may severely influence the geometry of individual Cu(II) complexes or even the crystal lattice geometry of paramagnetic salts, and are usually classified in terms of the Jahn–Teller and pseudo-Jahn–Teller effects. Detailed treatment of the Jahn–Teller type coupling have appeared in several textbooks and review articles [12–14], therefore only a brief outline of the problem related to the $[Cu(H_2O)_6]$ complexes will be given here.

In octahedral Cu(II) complexes with identical ligands the vibronic coupling appears between doubly degenerate electronic E_g and vibrational ε_g functions

$(E \otimes \varepsilon)$. The form of the vibronic Hamiltonian is

$$\mathcal{H}_{\text{vibr}} = \mathcal{H}_0 + \mathcal{H}_{\text{JT}} + \mathcal{H}_{\text{ST}}.$$

$\mathcal{H}_0$ is a pure vibrational Hamiltonian of the undistorted geometry containing harmonic and anharmonic terms

$$\mathcal{H}_0 = [(h\nu/2)(P_\Theta^2 + p_\varepsilon^2 + Q_\Theta^2 + Q_\varepsilon^2) + K_3 Q_\Theta (Q_\Theta^2 - 3Q_\varepsilon^2)] \cdot I,$$

where $h\nu$ is ε_g vibration energy in the absence of the Jahn–Teller effect typically equal to about 300 cm^{-1} in copper(II) Tutton salts, P_i and Q_i are conjugate momenta and normal coordinates, and K_3 is an anharmonicity constant. I is an unity operator of the form

$$I = \begin{pmatrix} 1 & 0 \\ 0 & 1 \end{pmatrix}.$$

$\mathcal{H}_0$ determines the shape of the potential energy surface in Q_i-space when no vibronic coupling operates.

The Jahn–Teller Hamiltonian $\mathcal{H}_{\text{JT}}$ describes the linear, first-order Jahn–Teller coupling with coupling constant A_1, and nonlinear, second-order Jahn–Teller coupling with coupling constant A_2:

$$\mathcal{H}_{\text{JT}} = A_1(Q_\Theta \delta_z - Q_\varepsilon \delta_x) + A_2[(Q_\Theta^2 - Q_\varepsilon^2)\delta_z + 2Q_\Theta Q_\varepsilon \delta_x],$$

where δ_x, δ_z are pseudospin operators:

$$\delta_x = \begin{pmatrix} 0 & 1 \\ 1 & 0 \end{pmatrix}, \qquad \delta_z = \begin{pmatrix} 1 & 0 \\ 0 & -1 \end{pmatrix}.$$

Assuming of a harmonic vibrational potential ($K_3 = 0$) and taking of only the linear Jahn–Teller coupling term give rise to the well-known "Mexican hat" potential surface. In this, the $Cu(H_2O)_6$-octahedron fluctuates between the various conformations of D_{4h} and D_{2h} symmetry generated by linear combinations of $Q_\Theta = \rho\cos\phi$ and $Q_\varepsilon = \rho\sin\phi$ being the components of the Jahn–Teller active vibrational mode. The potential energy minimum may be considered to take the form of a circular well of the Jahn–Teller radius ρ_0 which was estimated to be about $\rho_0 = 0.02$ nm for $[Cu(H_2O)_6]^{2+}$ complexes [15]. The spin coupling and orthorhombic component of the crystal field can deform the Mexican hat surface as is shown for the cross-section along Q_Θ-coordinate in Fig. 2. The Jahn–Teller stabilization energy E_{JT} marked in Fig. 2 is large as compared to the vibrational energy $h\nu$ in Cu(II)–O_6 coordination and was estimated to be of about 1800 cm^{-1} [16]. The linear coupling constant A_1 value is related to the E_{JT} by the approximate expression $A_1 = (2h\nu E_{\text{JT}})^{1/2}$ [12] and can be estimated to be of about $A_1 = 1000$ cm^{-1}.

When the higher-order Jahn–Teller term and vibronic anharmonicity are taken into account, the minimum potential energy at ρ_0 becomes dependent on the angular coordinate, causing the perimeter of the Mexican hat to become "warped", with three minima corresponding to three possible directions of tetragonal elongation of the octahedra, while the three saddle points connecting these minima represent compressed configurations. The barrier height 2β between equivalent wells can be estimated as $\beta \approx A_2\rho_0^2$ with the value varying from 20 to 350 cm^{-1} [17].

The behaviour of a system observed by EPR depends on a relative value of the zero-point vibrational energy ($h\nu$) of the system and the height of the barrier

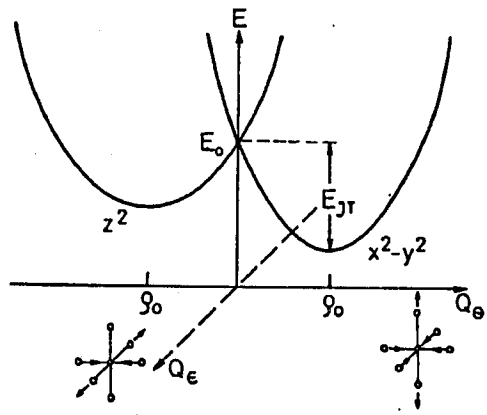

Fig. 2. The adiabatic potential surface ("Mexican hat") cross-section along Q_Θ direction in the case of the linear Jahn–Teller effect. An asymmetry in $E_{x^2-y^2}$ and E_{z^2} is due to an orthorhombic crystal field distortion.

(2β). If $h\nu \ll 2\beta$, then the ground states are strongly localized in the individual minima (static Jahn–Teller effect) and three superimposed axial EPR spectra from the individual wells are observed in a single crystal. At higher temperatures the system may be delocalized between wells as well as the tunnelling transition rate between wells can increase leading to a motionally averaged EPR spectrum.

In most of real situations, however, ligand molecules situated along the x, y, and z axes of the CuO_6-complex are not equivalent, since they are involved in different intermolecular interactions. This can have a significant influence on the potential energy surface and EPR behaviour. It can be described in terms of host lattice strains by the Hamiltonian

$$\mathcal{H}_{ST} = S_\Theta \delta_z - S_\epsilon \delta_x$$

where S_Θ and S_ϵ are the tetragonal and orthorhombic components of the strain, respectively. The strains produce differences in the energy between potential wells, and the strain effect can be especially large for dynamic Jahn–Teller systems with $h\nu \gg 2\beta$ even at low temperatures and for small strain values.

The exact energy levels and wave functions of the $[Cu(H_2O)_6]^{2+}$ complex can be obtained by diagonalization of the matrix of the vibronic Hamiltonian $\mathcal{H}_{vibr}$ in a basis of a truncated set of vibronic functions. This basis consists of two $E_g(d_{x^2-y^2}, d_{z^2})$ metal orbital wave functions and $N = (1/2)(n_\nu + 1)(n_\nu + 2)$ two-dimensional harmonic oscillator wave functions of the ε_g-vibration up to the level n_ν [18]. Detailed calculations were performed for Cu(II) doped Tutton salts [18] and fitted to experimental EPR and optical spectroscopy data. The one-dimensional cross-section of the potential surface obtained for $(NH_4)_2Zn(SO_4)_2 \cdot 6H_2O$:Cu(II) is shown in Fig. 3 together with plots of the lowest vibronic levels and vibronic probability functions for the parameters: $h\nu = 300\ cm^{-1}$, $A_1 = 900\ cm^{-1}$, $A_2 = 32\ cm^{-1}$, $S_\Theta = -550\ cm^{-1}$, and $S_\epsilon = 120\ cm^{-1}$ [18].

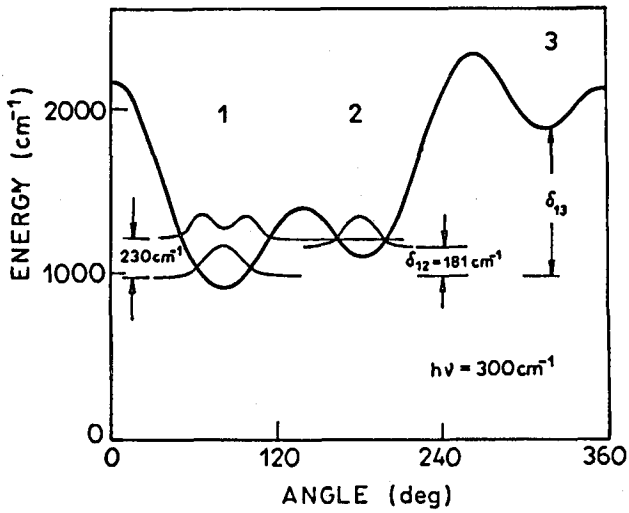

Fig. 3. The adiabatic potential surface cross-section along the Jahn–Teller perimeter ρ_0 calculated for Cu(II) doped $(NH_4)_2Zn(SO_4)_2 \cdot 6H_2O$ with parameters $h\nu = 300$ cm^{-1}, $A_1 = 900$ cm^{-1}, $A_2 = 33$ cm^{-1}, $S_\Theta = -550$ cm^{-1}, $S_\epsilon = 120$ cm^{-1} [18].

The dominant effect of the tetragonal component S_Θ of the lattice strain is clearly seen in Fig. 3, and it can be related to the hydrogen bonds between coordinated H_2O molecules and surrounding ions. The relatively large difference between minima of energy in the three potential wells dominates the temperature behaviour of EPR parameters of the system. At liquid helium temperature the complex is localized in the lowest well and a static rhombic EPR spectrum is observed. When temperature raises, vibronic effects appear in the spectrum but they are less pronounced as compared to the lattice unperturbed systems. The two lowest g-factors g_1 and g_2 become to be temperature dependent and tend towards their average value $(g_1 + g_2)/2$, and moreover, for isolated $[Cu(H_2O)_6]^{2+}$ complexes in diamagnetic lattice the hyperfine splittings are averaged with hyperfine pattern indicating a characteristic temperature dependent alteration in the line width values. These vibronic effects can be described equally well in terms of two distinctly different models.

In the Silver–Getz model [19] it is assumed that increase in temperature results in the population of 2 and 3 wells with a fast transitions between all three wells. The EPR g and A values are given by a weighted average of the Boltzmann population of the three lowest energy levels in the three potential wells. Moreover, it is assumed that the EPR parameters of the three wells are identical except for an interchange of the x, y, and z axes. An excellent agreement with experimental results for Cu(II) in zinc Tutton salt was found both for g and A values assuming the two lower wells population with energy difference $\delta_{12} = 75$ cm^{-1} and energy barrier $2\beta = 120$ cm^{-1} [19].

An alternative model was proposed by Riley and Hitchman [18]. In this model the temperature dependence of the EPR parameters is due not to exchange between different static distortions of the Cu(II) complex but to a Boltzmann distribution over the vibronic levels on the potential surface of the deepest well. Each vibronic level has its own set of g-factors and a rapid vibronic relaxation gives an averaging g-tensor. This approach has been successfully applied to the interpretation of the g-factor temperature behaviour of the $[Cu(H_2O)_6]^{2+}$ in diamagnetic Tutton salt crystals with parameters presented in Fig. 3.

Phenomenologically, both models as applied to the Tutton salts are two-level models which cannot be differenced definitely from EPR data although they lead to different values of the vibronic parameters. The g-factor temperature dependence can be described as resulting from the ground state wave function

$$\Psi = a|x^2 - y^2\rangle + b|z^2\rangle, \qquad a^2 + b^2 = 1$$

with a and b coefficients being temperature dependent due to the vibronic coupling. It seems, however, that the both approaches should be applied simultaneously for a description of the CuX_6 complexes.

The above described vibronic behaviour of isolated Jahn–Teller centres can be more complicated for pure Cu(II) compounds because of a cooperative elastic interaction between the Cu(II) ions (cooperative Jahn–Teller effect). In doped crystals the lattice strains are essentially temperature independent whereas in Cu(II) compounds a change in a complex geometry associated with an excitation to higher vibronic level will alter the environment of its neighbours. Thus a fixed set of energy levels may be no longer valid to describe the temperature behaviour of the system. This problem is not very well recognized yet, although an influence of the cooperative Jahn–Teller effect on magnetic properties of Cu(II) coordination compounds was studied for model systems [20, 21].

4. Results

Single crystal EPR spectrum of $(NH_4)_2Cu(BeF_4)_2 \cdot 6H_2O$ consists of two resonance lines from the two magnetically inequivalent Cu(II) sites. The peak-to-peak line width value varies from 7 mT to 15 mT depending on the crystal orientation with the line shape being Gaussian for the broadest lines and Lorentzian for the narrowest lines. Both the resonance field (g-factors) values and line width values are affected by temperature as it is shown in Fig. 4. The shape of the spectrum and the line positions are not disturbed by an exchange coupling between copper(II) ions, as is generally observed in Cu(II) compounds, since the coupling was unexpectedly found to be equal to zero in our previous studies [11]. The angular variations of the resonance field plotted in Fig. 4 were least-squares fitted to the g^2-tensor equation

$$g^2(\Theta) = \alpha + \beta\cos(2\Theta) + \gamma\sin(2\Theta)$$

and after a zero-angle correction the g^2-tensors for complexes 1 and 2 were formed. By diagonalization the principal g-factors and direction cosines of the principal x, y, z axes were obtained. These data are collected in Table. The solid lines in

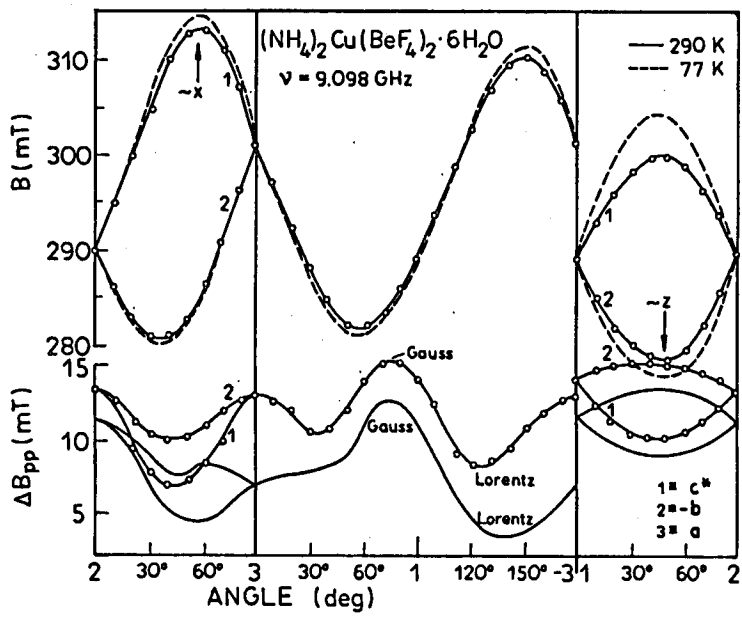

Fig. 4. Angular variations of the resonance field B and line width ΔB_{pp} in three planes of the reference system $1 = c^*$, $2 = -b$, $3 = a$, measured at room temperature and liquid nitrogen temperature. The inequivalent complexes 1 and 2 are marked consistently with the crystal structure (Fig. 1). Approximate positions of the local x and z axes are shown.

$B(\Theta)$ plots (Fig. 4) are theoretical plots with data from Table, and the principal axes are marked for complex 1 in Fig. 1.

The crystal and molecular structural data for the $(NH_4)_2Cu(BeF_4)_2 \cdot 6H_2O$ are unknown, but we can compare our EPR results with the structure [9] and EPR data [22] for the $(NH_2)_2Cu(SO_4)_2 \cdot 6H_2O$ crystal. The comparison is done in Table. The room temperature g-factors are slightly different in both crystals because of different temperature behaviour. The principal axes directions are very close in both compounds and our data fits perfectly to the Cu–O directions. It is a clear evidence that the sulphate and fluoroberyllate copper(II) ammonium Tutton salts are isostructural and particularly the $[Cu(H_2O)_6]^{2+}$ octahedra are elongated along the Cu–O(7) bond (z axis) in the both crystals, opposite to alkali metal Tutton salts. The small difference in the unit cell parameters (see introductory section) can be due to stronger hydrogen bonds in the fluoroberyllate crystal because of greater electronegativity of F as compared to O, as it was observed in $(NH_4)_2Ni(BeF_4)_2 \cdot 6H_2O$ [10].

The g-factors are temperature dependent in our crystal but the principal axes directions are not affected by temperature. The $g(T)$ dependencies were measured along principal x, y, z axes and are shown in Fig. 5. The g_x value slowly linearly increases with temperature whereas g_z and g_y tend symmetrically to their average

TABLE

EPR and structural data of two copper(II) ammonium Tutton salts at room temperature.

$(NH_4)_2Cu(SO_4)_2 \cdot 6H_2O$							
Cu–O bonds [nm]	Angle to the axis: [deg]			g-factor	Angle to the axis: [deg]		
	a	b	c^*		a	b	c^*
Cu–O(7) = 0.2216	53.9	49.5	61.2	$g_z = 2.360$	57.9	47.8	59.0
Cu–O(8) = 0.2078	139.1	49.6	84.9	$g_y = 2.218$	143.5	52.4	89.0
Cu–O(9) = 0.1962	106.0	114.3	29.7	$g_x = 2.071$	107.0	125.4	31.1

$(NH_4)_2Cu(BeF_4) \cdot 6H_2O$			
g-factor[1]	Angle to the axis: [deg]		
	a	b	c^*
$g_z = 2.402$	53.8	50.3	60.5
$g_y = 2.163$	140.0	50.5	84.7
$g_x = 2.064$	104.7	115.6	30.1

[1] Errors ±0.001.

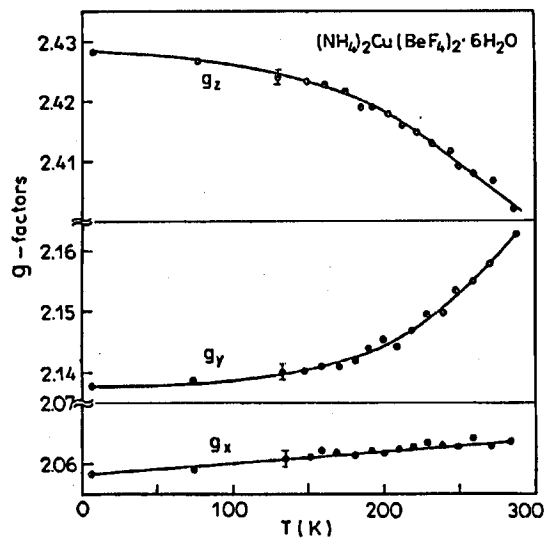

Fig. 5. Temperature dependence of the g-factors in $(NH_4)_2Cu(BeF_4)_2 \cdot 6H_2O$ crystals measured along Cu–O(7) bond (z axis), Cu–O(8) bond (y axis) and Cu–O(9) bond (x axis).

value. For the low-temperature rigid limit the g-factor values are

$$g_z = 2.428, \qquad g_y = 2.138, \qquad g_x = 2.058.$$

The line width value decreases on cooling along all crystal directions. This is shown along z and x axis in Fig. 6. Since the exchange coupling between inequiv-

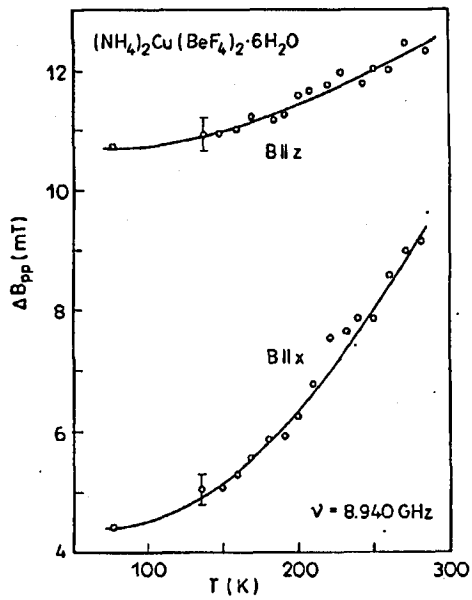

Fig. 6. Temperature dependence of the peak-to-peak line width along z and x principal g-tensor axes. The line shape is approximately Gaussian at z axis but is Lorentzian at x axis.

alent Cu(II) sites is negligible in the crystal, the line width value is determined by non-resolved hyperfine structure near the z axis, where the largest hyperfine splitting is expected, and is determined by spin-relaxation processes near x axis where the hyperfine splitting is minimal. Thus the line narrowing on cooling along x axis is due to a shortening of the spin-relaxation time, whereas a much smaller narrowing along z-axis direction is observed.

5. Discussion

The measured g-factor values in $(NH_4)_2Cu(BeF_4)_2 \cdot 6H_2O$ and their temperature behaviour are typical of Cu(II) in Tutton salts. However, the $g(T)$ variation rate is much smaller as compared to the Cu(II) doped diamagnetic Tutton salts. It is clearly seen in Fig. 7 where the data for $Cs_2Cu(ZrF_6)_2 \cdot 6H_2O$ [23] are also included. We are not able to compare our data to those in isostructural $(NH_4)_2Cu(SO_4)_2 \cdot 6H_2O$ crystal, since only the limited EPR data are available (Fig. 7) despite of a long history of the problem.

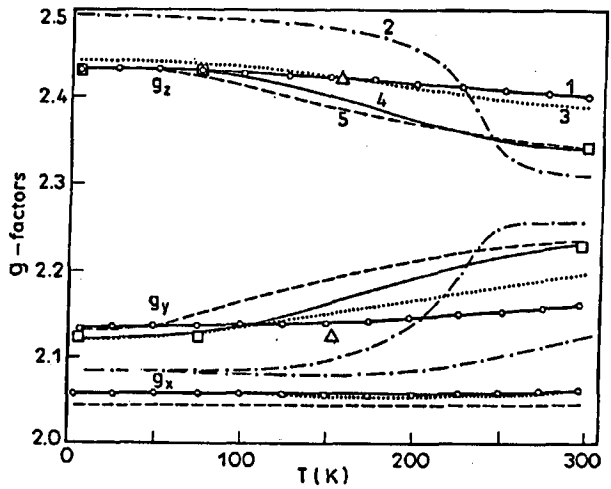

Fig. 7. Temperature variations of the g-factors for two Cu(II) compounds: 1 — $(NH_4)_2Cu(BeF_4)_2 \cdot 6H_2O$, 2 — $Cs_2Cu(ZrF_6)_2 \cdot 6H_2O$ [23], and for three Cu(II) doped "zinc" Tutton salts [7]: 3 — $Cs_2Zn(SO_4)_2 \cdot 6H_2O$, 4 — $(NH_4)_2Zn(SO_4)_2 \cdot 6H_2O$, 5 — $Rb_2Zn(SO_4)_2 \cdot 6H_2O$. The available g-factors for $(NH_4)_2Cu(SO_4)_2 \cdot 6H_2O$ at limited temperatures, are also presented: □ — from Ref. [7], △ — from Ref. [22].

A characteristic feature of $g_i(T)$ dependencies is a small temperature variation of the g_x value which appears along the shortest Cu–O(9) bond, and a tendency to the averaging of the two largest g values when temperature increases.

In general, the g-factor temperature behaviour can be described by the equation

$$g_z(T) = \frac{N_1}{N} g_{z1} + \frac{N_2}{N} g_{y2} + \frac{N_3}{N} g_{x3},$$

$$g_y(T) = \frac{N_1}{N} g_{y1} + \frac{N_2}{N} g_{z2} + \frac{N_3}{N} g_{y3},$$

$$g_x(T) = \frac{N_1}{N} g_{x1} + \frac{N_2}{N} g_{x2} + \frac{N_3}{N} g_{z3},$$

where $N = N_1 + N_2 + N_3$, and N_1, N_2, N_3 are the populations of the first, second and third potential wells in the Silver–Getz model or the populations of the ground, first excited, and second excited vibronic states in the Riley–Hitchman model, as described in the theoretical section.

The g_{ik} are the rigid values of g_{zk}, g_{yk}, g_{xk} in the k-th wall or on the k-th vibronic level. Since g_x is very weakly temperature dependent, then in good approximation $N_3 = 0$ and we have a two-level problem. To find the N_1 and N_2 values from experimental data the g-factor for $k = 2$ must be known, whereas only g_{z1} and g_{y1} for the ground state in the first well are known. The g_{z2} and g_{y2} values, in general, can be different from g_{z1} and g_{y2}, which should result in asymmetrical

temperature variations of the effective g_z and g_y values. However, in all Tutton salts the g_z and g_y value tend symmetrically to their average value in the whole temperature range. It is possible only when the local g-factors are identical in both wells, or on both vibronic levels, i.e. $g_{z1} = g_{z2}$ and $g_{y1} = g_{y2}$. It proves that $[Cu(H_2O)_6]^{2+}$ octahedra deformations are due mainly to the Jahn–Teller effect. Taking $N = 1$ we have in our case

$$g_z(T) = N_1 g_{z1} + (1 - N_1) g_{y1}, \qquad g_y(T) = N_1 g_{y1} + (1 - N_1) g_{z1},$$

which allows one to determine, independently from this two equations, the $N_1(T)$ dependence using experimental $g_z(T)$, $g_y(T)$ data and the rigid limit values $g_{z1} = 2.428$, $g_{y1} = 2.138$. Assuming the Boltzmann population $N_1/N_2 = \exp(\delta_{12}/kT)$, where δ_{12} is the energy level splitting, one can find the δ_{12} value as a function of temperature. The result is shown in Fig. 8 and compared with δ_{12} values calculated in analogous manner for the four zinc ammonium Tutton salts of alkali metals [7].

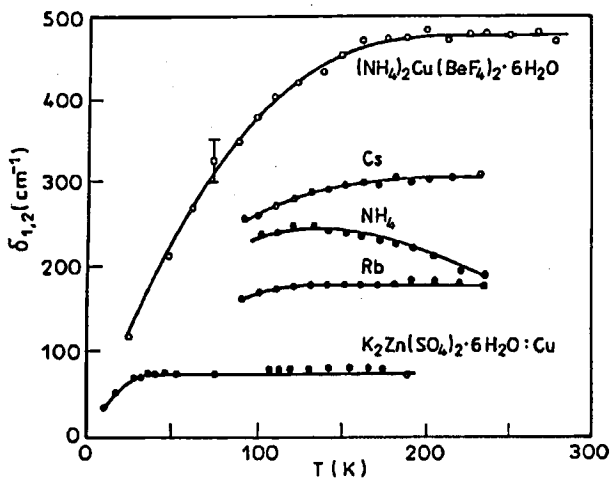

Fig. 8. Temperature dependence of the energy difference δ_{12} between the ground state and the excited state obtained from the two-level model as applied to the EPR g-factor temperature variations for $(NH_4)_2Cu(BeF_4)_2 \cdot 6H_2O$ and for four Cu(II) doped "zinc" Tutton salts $X_2Zn(SO_4)_2 \cdot 6H_2O$, X = K, Rb, NH_4, Cs [7].

The δ_{12} value is of about 100 cm^{-1} at 25 K and increases monotonically to about 480 cm^{-1} at room temperature. An accuracy of the g-factor determination does not allow one to find the δ_{12} behaviour below 25 K. The $\delta_{12}(T)$ dependence in $(NH_4)_2Cu(BeF_4)_2 \cdot 6H_2O$ is quite different from that for the Cu(II) doped Tutton salts. A weak $\delta_{12}(T)$ dependence observed in the doped salts can be attributed to the existence of the higher excited vibronic states as was suggested in EPR studies of Cu(II) in $ZnTiF_6 \cdot 6H_2O$ [24], or can appear when both the excited levels in the deepest well and the ground state of the second well are simultaneously thermally populated, or when the third potential well becomes to be populated. Moreover, a small effect can be produced by the thermal lattice expansion affecting the strain parameters.

However, the strong increase in δ_{12} value in $(NH_4)_2Cu(BeF_4)_2 \cdot 6H_2O$ cannot be explained by these effects. A similar large increase in the δ_{12} value from about 200 m^{-1} at 4.2 K to 300 cm^{-1} at 300 K was reported for $[Cu([9]aneN_3)_2][Cu(CN)_3] \cdot 2H_2O$ [25].

6. Conclusions

Our results clearly show that it is impossible to describe the vibronic g-factor behaviour in $(NH_4)_2Cu(BeF_4) \cdot 6H_2O$ crystal in terms of the simple two-level excitation model which assumes temperature independent adiabatic potential surface and constant vibronic levels splittings. This model is here only a very crude approximation, although it was found to be quite appropriate in Cu(II) doped diamagnetic crystals. It suggests that an inadequacy of the model as applied to paramagnetic crystals is due to the cooperative Jahn–Teller type interaction between copper(II) ions. This long-distance elastic interaction transmitted through the lattice phonons (vibrons) is expected to hinder the jumps between potential wells which can be described as temperature induced modifications of the adiabatic potential surface. As a result the temperature averaging of the g-factors can go much slowly at low temperatures as compared to Cu(II) doped crystals, and then rapidly an average g-value can be reached as observed in $Cs_2Cu(ZrF_6)_2 \cdot 6H_2O$ [23] (Fig. 7) or even a jump-like behaviour can appear as has been found in $K_2Cu(DP)_2 \cdot 7H_2O$ [26]. Such behaviour as well as an insensitivity of the g-factors to temperature in other Cu(II) Tutton salts seems to be attributed to the cooperative Jahn–Teller effect. However, the problem is far from being satisfactorily explained or even theoretically described. Moreover, in most of Cu(II) compounds the exchange coupling and its temperature dependence [27] will disturb pure vibronic effects and complicate an analysis of EPR spectra by a disturbance the spectral shape and a shift of the g-factor values.

References

[1] B.J. Hathaway, W. Hewat, *J. Solid State Chem.* **51**, 364 (1984).

[2] B. Bleaney, R.P. Penrose, B.I. Plumpton, *Proc. R. Soc. Lond. A* **198**, 406 (1949).

[3] D. Reinen, C. Friebel, in: *Structure and Bonding* Vol. 37, Springer, Berlin 1979, p. 1.

[4] Yu.V. Yablokov, A.E. Usachev, T.A. Ivanova, in: *Radiospectroscopy of Condensed Matter*, Ed. M.M. Zaripov, Nauka, Moscow 1990, p. 147.

[5] B.J. Hathaway, in: *Structure and Bonding*, Vol. 57, Springer-Verlag, Berlin 1984, p. 55.

[6] N.W. Alock, M. Duggan, A. Murray, S. Tyagi, B.J. Hathaway, A. Hewat, *J. Chem. Soc. Dalton Trans.* 7, (1984).

[7] V.E. Petrashen, Yu.V. Yablokov, R.L. Davidovich, *Phys. Status Solidi B* **101**, 117 (1980).

[8] S. Tedenai, A. Cot, *C.R. Acad. Sci.* 1163 (1970).

[9] E.N. Maslen, K.J. Watson, F.H. Moore, *Acta Crystallogr. B* **44**, 102 (1988).

[10] H. Montgomery, *Acta Crystallogr. B* **36**, 2121 (1982).

[11] S.K. Hoffmann, M. Gomółka-Marciniak, *Solid State Commun.* **86**, 63 (1993).

[12] I.B. Bersuker, *The Jahn–Teller Effect and Vibronic Interactions in Modern Chemistry*, Nauka, Moscow 1987 (in Russian), Plenum Press, New York 1984 (in English).

[13] *The Dynamical Jahn–Teller Effect in Localized Systems*, Eds. Yu.E. Perlin, M. Wagner, North-Holland, Amsterdam 1984.

[14] D. Reinen, M. Atanasov, *Magn. Res. Rev.* **15**, 167 (1991).

[15] R. Akesson, L.G.M. Pettersson, M. Sandstrom, U. Wahlgren, *J. Phys. Chem.* **96**, 150 (1992).

[16] H. Bill, in Ref. [13], Ch. 13.

[17] M.J. Riley, M.A. Hitchman, D. Reinen, G. Steffen, *Inorg. Chem.* **27**, 1924 (1988).

[18] M.J. Riley, M.A. Hitchman, A.W. Mohammed, *J. Chem. Phys.* **87**, 3766 (1987).

[19] B.L. Silver, D. Getz, *J. Chem. Phys.* **61**, 638 (1974).

[20] B.G. Vekhter, *Fiz. Tverd. Tela* **28**, 2406 (1986).

[21] K.I. Kugel, D.I. Khomskii, *Usp. Fiz. Nauk* **136**, 621 (1982).

[22] F.E. Mabbs, J.K. Porter, *J. Inorg. Nucl. Chem.* **35**, 3219 (1973).

[23] M.W. Eremin, A.Yu. Zavidonov, W.E. Petrashen, Yu.V. Yablokov, R.L. Davidovich, *Fiz. Tverd. Tela* **29**, 3426 (1987).

[24] R.S. Rubins, J.E. Drumheller, *J. Chem. Phys.* **86**, 6660 (1987).

[25] P. Chaudchuri, K. Oder, K. Wieghardt, J. Weiss, J. Reedijk, H. Hinrichs, J. Wood, A. Ozarowski, H. Stratemeier, D. Reinen, *Inorg. Chem.* **25**, 2951 (1986).

[26] A.Yu. Leontyev, G.A. Popowich, Yu.V. Yablokov, *Koord. Khimiya* **11**, 1333 (1985).

[27] S.K. Hoffmann, W. Hilczer, *Inorg. Chem.* **30**, 2210 (1991).